Rab5 modulates aggregation and toxicity of mutant huntingtin through macroautophagy in cell and fly models of Huntington disease

Brinda Ravikumar[1], Sara Imarisio[1,2], Sovan Sarkar[1], Cahir J. O'Kane[2] and David C. Rubinsztein[1,*]

[1]Department of Medical Genetics, Cambridge Institute for Medical Research, Wellcome/MRC Building, Addenbrooke's Hospital, Hills Road, Cambridge, CB2 0XY, UK
[2]Department of Genetics, University of Cambridge, CB2 3EH, UK
*Author for correspondence (e-mail: dcr1000@hermes.cam.ac.uk)

Accepted 21 February 2008
Journal of Cell Science 121, 1649-1660 Published by The Company of Biologists 2008
doi:10.1242/jcs.025726

Summary

Huntington disease (HD) is caused by a polyglutamine-expansion mutation in huntingtin (HTT) that makes the protein toxic and aggregate-prone. The subcellular localisation of huntingtin and many of its interactors suggest a role in endocytosis, and recently it has been shown that huntingtin interacts indirectly with the early endosomal protein Rab5 through HAP40. Here we show that Rab5 inhibition enhanced polyglutamine toxicity, whereas Rab5 overexpression attenuated toxicity in our cell and fly models of HD. We tried to identify a mechanism for the Rab5 effects in our HD model systems, and our data suggest that Rab5 acts at an early stage of autophagosome formation in a macromolecular complex that contains beclin 1 (BECN1) and Vps34. Interestingly chemical or genetic inhibition of endocytosis also impeded macroautophagy, and enhanced aggregation and toxicity of mutant huntingtin. However, in contrast to Rab5, inhibition of endocytosis by various means suppressed autophagosome-lysosome fusion (the final step in the macroautophagy pathway) similar to bafilomycin A1. Thus, Rab5, which has previously been thought to be exclusively involved in endocytosis, has a new role in macroautophagy. We have previously shown that macroautophagy is an important clearance route for several aggregate-prone proteins including mutant huntingtin. Thus, better understanding of Rab5-regulated autophagy might lead to rational therapeutic targets for HD and other protein-conformation diseases.

Supplementary material available online at
http://jcs.biologists.org/cgi/content/full/121/10/1649/DC1

Key words: Huntington disease, Autophagy, Rab5

Introduction

Huntington disease (HD) is a late-onset inherited neurodegenerative condition caused by an expansion of CAG trinucleotide repeats (>35 repeats) in exon 1 of the IT15 gene. The mutation results in the production of an abnormally long polyglutamine (polyQ) tract in the N-terminus of the huntingtin (HTT) protein (Rubinsztein, 2002). Full-length mutant huntingtin undergoes several proteolytic cleavages, which give rise to N-terminal fragments comprising the first 100-150 residues containing the expanded polyQ tract. These N-terminal fragments are also the toxic species found in aggregates seen in HD mouse models and human brains (Lunkes et al., 2002). Thus, HD pathogenesis is frequently modelled with fragments of exon 1 that contain expanded polyQ repeats, which cause toxicity and the formation of aggregates in cell models and in vivo (Rubinsztein, 2002).

A key pathway that regulates the degradation of aggregate-prone cytosolic proteins such as mutant huntingtin (both full-length and exon 1 forms) is macroautophagy – henceforth referred to simply as autophagy (Ravikumar et al., 2002; Ravikumar et al., 2004; Shibata et al., 2006). Wild-type huntingtin (full-length or exon 1) has a very low dependence on autophagy for its clearance. Autophagy, a process conserved from yeast to human, typically clears long-lived proteins and organelles by engulfing cytoplasmic contents in double-membrane structures called autophagosomes, which later fuse with lysosomes, where their contents are degraded (Klionsky and Ohsumi, 1999). It is believed that isolation membranes (phagophores) – which later give rise to autophagosomes – are formed at the phagophore-assembly site (also referred to as pre-autophagosomal structures, PAS) in yeast (Suzuki et al., 2001). PAS however have not been defined in mammalian autophagy. Several 'Atg' (autophagy) genes that regulate yeast autophagy have been identified, and many of these genes have mammalian orthologues. A protective role of autophagy has been implicated in some neurodegenerative disorders, cancers and infectious diseases (Rubinsztein et al., 2007). Conditional knockouts of the key autophagy genes *Atg5* or *Atg7* in the brains of mice result in a neurodegenerative phenotype caused by aberrant accumulation of ubiquitinated proteins (Hara et al., 2006; Komatsu et al., 2006). In addition to HD, where enhanced clearance of mutant huntingtin fragments through induction of autophagy attenuates toxicity caused by mutant huntingtin in cell, fly and mouse models (Ravikumar et al., 2002; Ravikumar et al., 2004), this pathway appears to be equally important for the clearance of several other intracellular proteins that cause neurodegeneration, including the A53T point mutation in α-synuclein that causes autosomal-dominant Parkinson disease (Berger et al., 2006; Ravikumar et al., 2002; Webb et al., 2003).

The subcellular localisation of huntingtin, the nature of many of its normal interactors and its indirect interaction with Rab5 through

HAP40 (Pal et al., 2006), suggested that it may have roles in endocytosis. Rab5, a member of the small GTPase family, is a key regulator of the early endocytic pathway in mammalian cells (Bucci et al., 1992; Stenmark et al., 1994). Accordingly, we initially tested the role of Rab5 in the regulation of toxicity of mutant huntingtin. We show that Rab5 inhibition enhances toxicity induced by mutant polyQ, whereas Rab5 overexpression attenuates mutant polyQ toxicity in HD cell and fly models. Our data suggest that Rab5, in addition to its role in endocytosis, modifies aggregation and toxicity of mutant huntingtin by having a novel role in the early stage of autophagosome formation. Interestingly, inhibition of endocytosis by a variety of means also influenced the toxicity of mutant huntingtin by inhibiting autophagy at a downstream step (autophagosome-lysosome fusion) that is distinct from Rab5 inhibition. A possible therapeutic approach for HD and other proteinopathies would thus be the enhancement of Rab5 activity.

Results and Discussion

Rab5 modifies polyglutamine toxicity and aggregation

We initially tested whether Rab5 can modify the toxicity of a mutant huntingtin exon 1 fragment with 74 polyQ repeats (Q74) (Narain et al., 1999) in COS-7 cells. Dominant-negative inhibition of Rab5 by overexpression of a GTP-binding-defective Rab5 mutant carrying a S34N point mutation (DN-Rab5) (Stenmark et al., 1994) increased the toxicity of Q74 (Fig. 1a), whereas overexpression of wild-type (WT) Rab5 or of a constitutively active (CA) Rab5 mutant carrying a Q79L mutation (CA-Rab5) (Stenmark et al., 1994) significantly decreased Q74-induced toxicity (Fig. 1a).

We then examined the effect of Rab5 on aggregation of mutant huntingtin. Aggregation of mutant huntingtin correlates with its expression levels (Narain et al., 1999). Also, the proportion of cells with inclusions formed by mutant huntingtin fragments generally correlates with its toxicity in cell culture models (although inclusions may not themselves be as toxic as diffusely distributed mutant huntingtin) (Arrasate et al., 2004; Ravikumar et al., 2002). DN-Rab5 increased Q74 aggregation, whereas CA-Rab5 and WT-Rab5 decreased the proportions of Q74-expressing cells with inclusions (Fig. 1b), mirroring the toxicity data (Fig. 1a). We next confirmed that the effects of DN-Rab5 were mirrored by depletion of endogenous Rab5 using RNA interference (RNAi). There are three isoforms of Rab5, namely Rab5A, Rab5B and Rab5C. Small interfering RNA (siRNA) that target individual Rab5 isoforms significantly increased Q74 aggregation, whereas simultaneous knockdown of all three isoforms increased Q74 aggregation even further (Fig. 1c, supplementary material Fig. S1). Thus, Rab5 modulation affects aggregation and toxicity of the mutant huntingtin fragments.

We next tested whether Rab5 can modify the toxicity of mutant huntingtin in vivo using a *Drosophila melanogaster* HD model. Fly photoreceptors that express a mutant huntingtin fragment with 120 polyQ repeats (Q120) exhibit degeneration that is not observed in flies that express the wild-type fragment with 23 polyQ repeats (Jackson et al., 1998). The *Drosophila* compound eye consists of many ommatidia, each comprising eight photoreceptor neurons with light-gathering parts called rhabdomeres, seven of which can be visualised by light microscopy using the pseudopupil technique (Franceschini and Kirschfeld, 1971). Neurodegeneration in the HD flies is progressive and is associated with a decrease in the number of visible rhabdomeres in each ommatidium with time (Jackson et al., 1998). We crossed the HD flies with flies transgenic for wild-type Rab5 fused to EGFP (Rab5-EGFP) and looked at the number of visible rhabdomeres in the double transgenic flies. Degeneration of photoreceptors due to Q120 overexpression was greatly rescued by overexpression of Rab5-EGFP (Fig. 1d).

Since our previous studies suggest that aggregation of mutant huntingtin can be regulated by autophagy (Ravikumar et al., 2002), we next tested whether the effects of Rab5 on Q74 aggregation are autophagy-dependent using either wild-type ($Atg5^{+/+}$) or autophagy-deficient Atg5-knockout ($Atg5^{-/-}$) mouse embryonic fibroblasts (MEFs) (Mizushima et al., 2001). As previously observed with autophagy inhibitors (Ravikumar et al., 2002), Q74 aggregation was higher in autophagy-incompetent $Atg5^{-/-}$ compared with $Atg5^{+/+}$ MEFs (Fig. 1e). We observed minimal Q74-induced cell death in the MEFs under the transfection conditions we used. As expected, overexpression of DN-Rab5 caused an increase and that of CA-Rab5 a decrease in Q74 aggregation in wild-type MEFs (Fig. 1f, left), similar to the results seen in COS-7 cells (Fig. 1b). However, overexpression of DN-Rab5 or CA-Rab5 had no effects on Q74 aggregation in autophagy-incompetent $Atg5^{-/-}$ MEFs (Mizushima et al., 2001) (Fig. 1f, right). Furthermore, Rab5 inhibition abrogated the ability of the autophagy enhancers, the mTOR inhibitor rapamycin or the inositol monophosphatase inhibitor L-690,330, which target mTOR-dependent or -independent pathways, respectively, to clear Q74 aggregates (Fig. 1g; supplementary material Fig. S2) (Ravikumar et al., 2002; Sarkar et al., 2005). This suggests that the effect of Rab5 on Q74 aggregation and toxicity were due to alterations in the autophagic pathway rather than its role in endocytosis.

Rab5 regulates autophagosome formation in mammalian cells

Since the above data suggest a possible role of Rab5 on autophagy, we tested whether Rab5 influenced the formation of autophagosomes. Two ubiquitin-like modifications are involved in the expansion and completion of autophagosome formation. The first involves conjugation of Atg12 to Atg5 in a reaction that requires Atg7 (E1-like) and Atg10 (E2-like). Atg5-Atg12 conjugates are localised onto the PAS and dissociate upon completion of autophagosome formation. The second modification involves conjugation of microtubule-associated protein 1 light chain 3 (hereafter referred to as LC3 and also known as MAP1LC3 or Atg8) to phosphatidylethanolamine (PE). LC3 (cytosolic) is cleaved at its C-terminus by Atg4 to form LC3-I. LC3-I is covalently conjugated to PE to form LC3-II, a process requiring the activities of Atg7 and Atg3. LC3-II (membrane associated) is specifically targeted to Atg5-Atg12-associated, expanded phagophores and remains associated with autophagosomes even after fusion with lysosomes, after which LC3-II can be delipidated and recycled. LC3 is the only known protein that specifically associates with autophagosomes and not with other vesicular structures (Kabeya et al., 2000). Thus, LC3-II levels correlate with the numbers of autophagic vacuoles, which can also be assessed by counting LC3-positive vesicles (Kabeya et al., 2000). We first tested the effect of Rab5 on LC3. Whereas, inhibition of Rab5 decreased the proportion of COS-7 cells with >20 LC3-labelled autophagic vesicles (Fig. 2a), overexpression of CA-Rab5 or WT-Rab5 significantly increased the proportion of cells with >20 LC3-positive autophagic vesicles (Fig. 2a). However, we did not observe any change in the size or morphology of the LC3 vesicles under any of the above conditions (data not shown). The above results also correlated with decrease (upon DN-Rab5 overexpression) or increase (upon CA-Rab5 or WT-Rab5 overexpression) with autophagosome-associated LC3-II levels on western blots when we blocked LC3-II clearance through inhibition

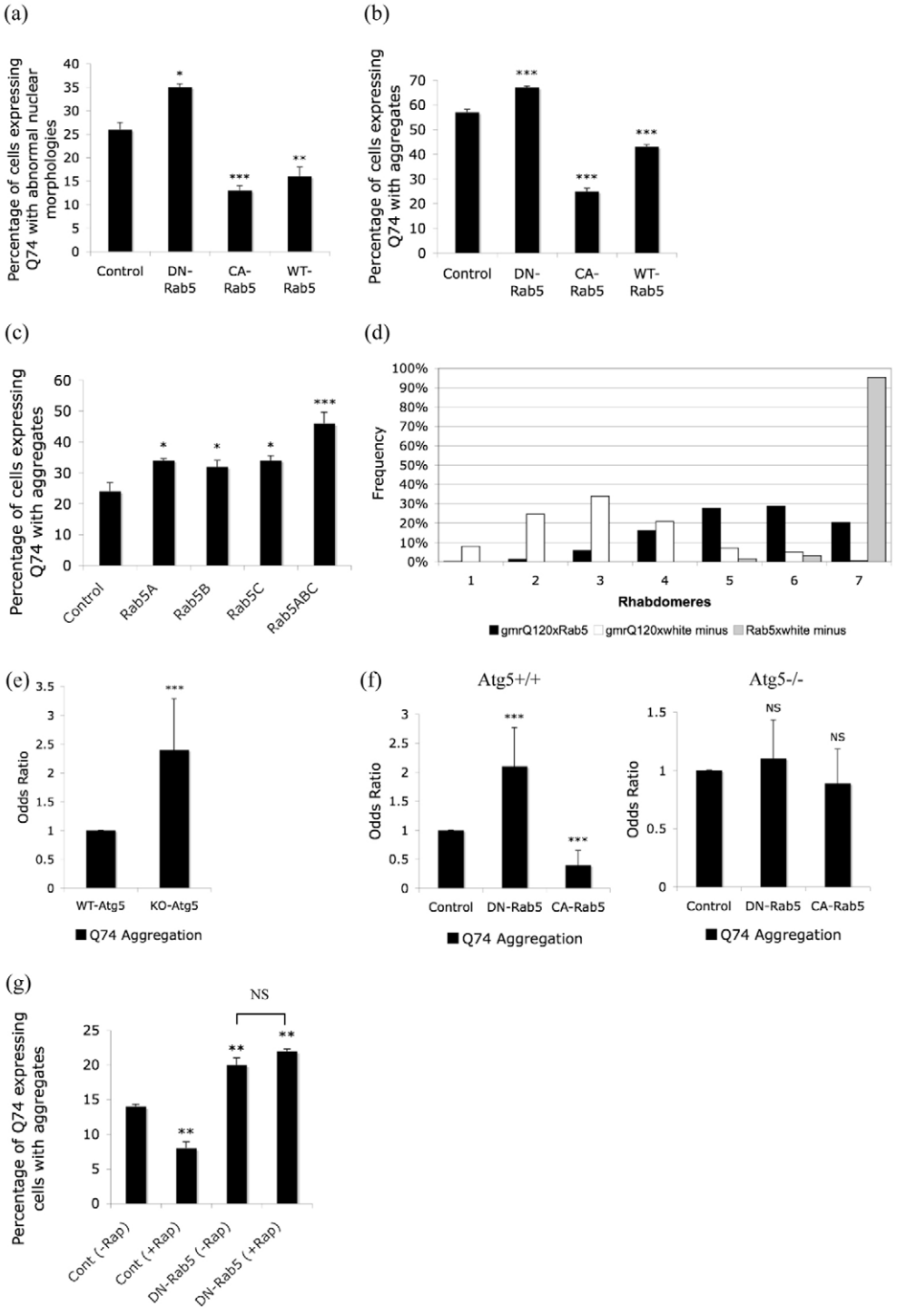

Fig. 1. Rab5 modulates the aggregation and toxicity of mutant huntingtin. (a) Quantification of GFP-expressing COS-7cells showing signs of cell death that had been transiently transfected with dominant-negative (DN), constitutive active (CA) or wild-type (WT) Rab5, or empty vector control, and the EGFP-tagged huntingtin exon 1 with 74 polyglutamine repeats (Q74) (at a 3:1 ratio) for 48 hours. ***P<0.0001, **P<0.001, *P<0.05. (b) Quantification of GFP-expressing COS-7 cells containing aggregates that were quantified for toxicity shown above. ***P<0.0001. (c) Quantification of GFP-expressing HeLa cells containing aggregates transiently transfected with siRNA targeting Rab5a, Rab5b, Rab5c or all three siRNA simultaneously (Rab5abc) for 72 hours, and also with EGFP-tagged huntingtin exon 1 with 74 polyglutamine repeats for the last 24 hours of the 72-hour siRNA transfection period. ***P<0.0001, *P<0.05. (d) Rab5 overexpression increases the numbers of rhabdomeres in ommatidia of mutant huntingtin-expressing flies. Frequency distribution of ommatidia with different numbers of rhabdomeres three days after eclosion (hatching) in progeny of flies that express mutant huntingtin exon 1 (gmrQ120) and that had been crossed to either a control stock (w^{1118}) (white minus; have huntingtin transgene only) or to Rab5-EGFP flies (have huntingtin and Rab5 transgenes). $P \leqslant 0.001$, t-test; $P \leqslant 0.001$, Mann-Whitney U test. The rhabdomere frequency of Rab5 flies crossed to a control stock is also shown. (e) Odds ratio of GFP-expressing cells with Q74 aggregates in wild-type ($Atg5^{+/+}$) vs Atg5 knockout ($Atg5^{-/-}$) MEFs. ***P<0.0001. (f) Odds ratio of Q74-expressing $Atg5^{-/-}$ (Atg5 knockout) or $Atg5^{+/+}$ (wild-type) MEF cells with aggregates, after transient transfection with dominant-negative Rab5 (DN-Rab5), constitutive active Rab5 (CA-Rab5) or empty vector control and EGFP-tagged huntingtin exon 1 with 74 polyglutamine repeats (Q74) (3:1 ratio) for 48 hours. ***P<0.0001. Odds ratios are given to compare pooled summary statistics across multiple independent experiments (see Materials and Methods). Control conditions are fixed at 1 in both cell lines to facilitate comparisons. (g) Quantification of GFP-expressing HeLa cells containing aggregates that had been transiently transfected with dominant-negative Rab5 (DN-Rab5) or empty vector (Cont) and huntingtin exon 1 with 74 polyglutamine repeats (Q74) (at a 3:1 ratio) for 48 hours and were either left untreated (–Rap) or treated with 0.2 μg/ml rapamycin (Rap) to induce autophagy. **P<0.001. Error bars in all graphs represent the s.e.m.

of autophagosome-lysosome fusion using bafilomycin A1 (BafA1) at 200 nM (Fig. 2b) (Sarkar et al., 2007). Further blockage of autophagosome-lysosome fusion through a BafA1-independent mechanism, using the dynein inhibitor erythro-9-[3-(2-hydroxynonyl)] adenine (EHNA), together with this dose of BafA1, does not increase LC3-II compared with using BafA1 alone (Sarkar et al., 2007). Results shown in Fig. 2b suggest that Rab5 increased autophagosome synthesis, rather than decreasing autophagosome-lysosome fusion and/or autophagosome degradation.

Rab5 and its effector Vps34 regulate early steps of autophagosome formation

Autophagosome formation begins with a nucleation step during which membranes of unknown origin form phagophores; these then

expand and fuse to form completed autophagosomes. The formation of autophagosome precursors is regulated by a macromolecular complex that contains phosphoinositide 3-kinase class 3 (Vps34 or PIK3C3), beclin 1 (BECN1, the human ortholog of yeast Atg6p), Atg14 and Vps15 (PIK3R4) (Kihara et al., 2001b). Vps34, which generates phosphatidylinositol-3-phosphate [PtdIns(3)*P*], directly interacts with beclin 1 (Kihara et al., 2001a). 3-methyl adenine (3MA) (Kovacs et al., 1998) or wortmannin (Blommaart et al., 1997) inhibit PI 3-kinases, including Vps34, and block autophagy by preventing the formation of autophagosomes. Conjugation of Atg12 with Atg5 initiates the elongation process. This conjugation however is not required for membrane targeting of Atg5, but is necessary for membrane elongation. This is followed by conjugation of PE to LC3-I to form LC3-II. Atg5-Atg12 conjugates colocalise with LC3-II on the PAS. Mutation of K130R in Atg5 ($Atg5^{K130R}$) inhibits its conjugation with Atg12; as a result, membranes with unconjugated $Atg5^{K130R}$ that do not colocalise with LC3-II accumulate upon autophagy induction (Mizushima et al., 2001). The Atg5-Atg12 conjugate only localises to phagophores and dissociates just before or after completion of autophagic vacuole formation (Mizushima et al., 2001). So Atg5 and Atg12 are not associated with completed autophagosomes.

To investigate how Rab5 influenced early steps in autophagosome formation, we investigated the distribution of GFP-tagged Atg5 (GFP-Atg5), a marker for autophagosomal precursor structures (George et al., 2000; Mizushima et al., 2001). Cells were

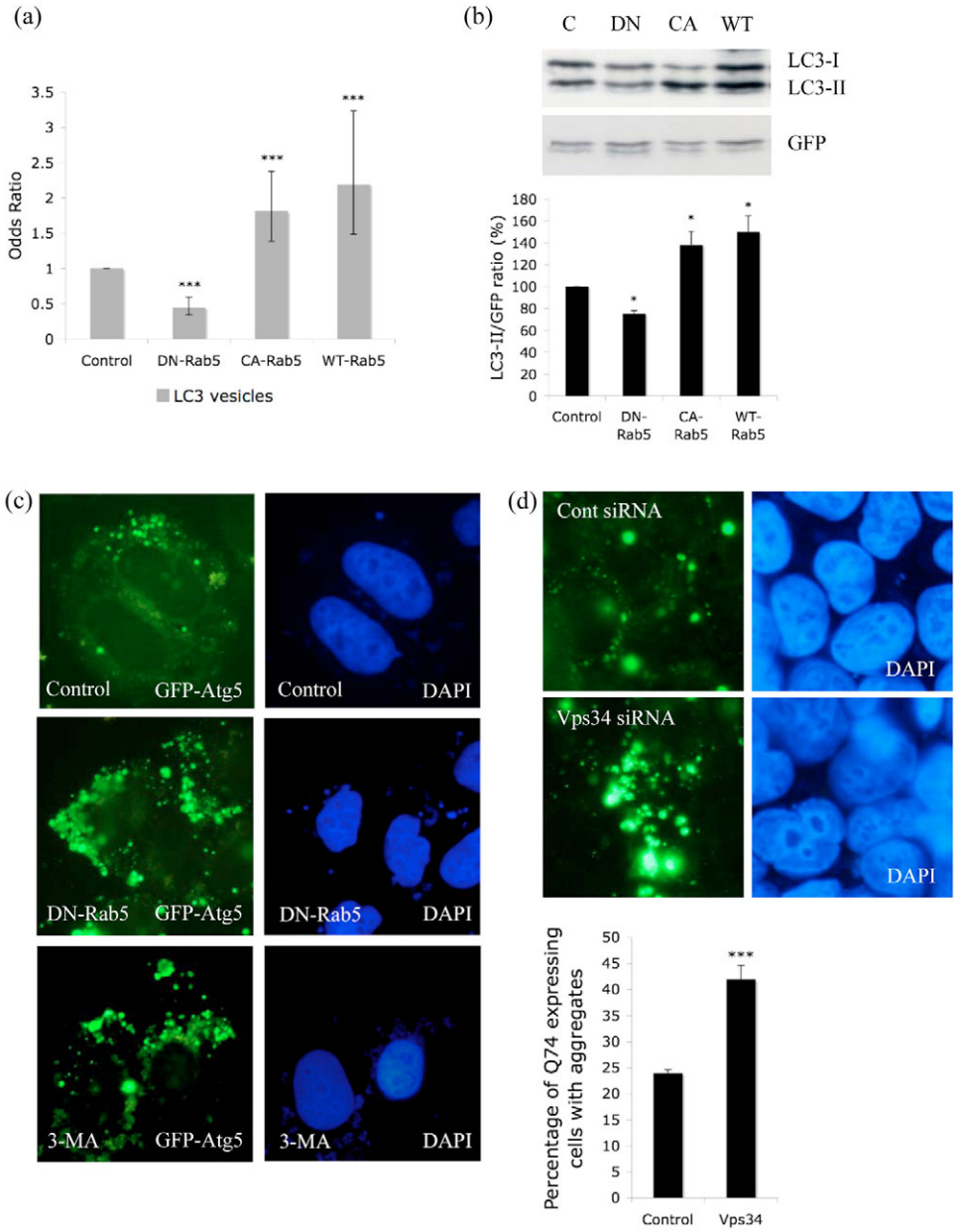

Fig. 2. (a) COS-7 cells were transiently transfected with empty vector (Control), DN-Rab5, CA-Rab5 or WT-Rab5 and GFP-LC3 or mRFP-LC3 (3:1 ratio) for 24 hours. GFP-positive or mRFP-positive cells with increased numbers of LC3-positive vesicles (>20 vesicles per cell) were counted. 29% of control cells had >20 vesicles per cell. ***P<0.0001. (b) Western blot analysis of COS-7 cells co-transfected with empty vector (C), DN-Rab5, CA-Rab5 or WT-Rab5 and Myc-LC3 for 24 hours in the presence of 200 nM bafilomycin A1 (treated for last 15 hours), using anti-Myc antibody. GFP was used as a transfection control. Representative image from three independent experiments; quantification of the band intensities from these experiments represented as LC3-II:GFP ratio is shown in the graph; *P<0.05. (c) Analysis of GFP-Atg5 structures (green) in HeLa cells transfected with control vector [either untreated or treated for 24 hours with 10 mM 3-methyladenine (3-MA)] or with dominant-negative Rab5 (DN-Rab5) and GFP-Atg5, after saponin extraction. Nuclei are shown in blue. An increased abundance of large punctate Atg5 structures can be noticed with DN-Rab5 and 3-MA treatment. (d) HeLa cells were transfected with siRNA targeting Vps34 or control siRNA for 48 hours after which GFP-Atg5 together with siRNA was transfected for further 24 hours. The cells were fixed following saponin extraction to visualise GFP-Atg5 (green) structures. Quantification of Q74-expressing HeLa cells with aggregates is shown in the graph. Cells were transiently transfected with control siRNA or siRNA targeting Vps34 for 48 hours and with HA-tagged huntingtin exon 1 containing 74 polyglutamine repeats for further 24 hours. ***P<0.0001. (e) Colocalisation of GFP-Atg5 structures (green) with Myc-tagged FYVE (red) in HeLa cells co-transfected with DN-Rab5, GFP-Atg5 and Myc-FYVE for 24 hours. (f) Colocalisation of GFP-Atg5 structures (green) with beclin 1 (red) in HeLa cells co-transfected with DN-Rab5, GFP-Atg5 and Flag-tagged wild-type (WT) beclin 1. (g) Colocalisation of endogenous Atg5 (red) and endogenous Rab5 (green) in HeLa cells treated with 3MA for 15 hours. In panels e-g we observed >30% colocalisation between GFP-Atg5 structures and saponin-extracted, membrane-associated, FYVE, beclin 1 or Rab5 in cells that expressed both of the respective proteins. (h) Colocalisation of GFP-Atg5 structures (green) with Atg12 (red) in HeLa cells co-transfected with DN-Rab5 and GFP-Atg5 and HA-tagged Atg12 for 24 hours. Nuclei labelled with DAPI are in blue.

permeabilised with saponin to remove soluble cytosolic contents and reveal membrane-associated GFP-Atg5. After Rab5 inhibition, we noted an increased abundance of large punctate Atg5 structures (Fig. 2c). These contrast with the smaller and less abundant Atg5 puncta seen in the great majority of untreated cells (Fig. 2c). We found similar results when we immunostained for endogenous Atg5 (supplementary material Fig. S3). In control cells, however, these structures were rare (Fig. 2c; supplementary material Fig. S3). Whereas saponin extraction precludes accurate quantitation (because it does not allow visualisation of transfected versus untransfected cells), we saw these Atg5 structures in 3% of all control cells and in about 12% of Rab5-inhibited cells (an ~fourfold increase, $P<0.001$ from triplicate slides).

Previous studies have shown that Rab5 interacts with and activates the PI 3-kinase Vps34 (Christoforidis et al., 1999). Thus, we tested whether Vps34 inhibition had similar effects to Rab5 inhibition. As with Rab5 inhibition, inhibition of Vps34 with the PI 3-kinase inhibitors 3MA (Fig. 2c; supplementary material Fig. S3) or wortmannin (data not shown) (which are both established blockers of autophagosome formation) or siRNA knockdown of Vps34 (Fig. 2d; supplementary material Fig. S4) resulted in increases of Atg5 structures. Similar to Rab5 inhibition, inhibition of Vps34 also increased the proportion of cells with Q74 aggregates, consistent with autophagy inhibition (Fig. 2d) (Ravikumar et al., 2002). To further characterise the Atg5 structures we tested whether they colocalised with other markers or proteins associated with phagophores. A subset of the punctate Atg5 structures colocalised with a PtdIns(3)*P* marker, Myc-FYVE (Fig. 2e) (Gaullier et al., 1998) and they also overlapped with beclin 1 (Fig. 2f) but did not colocalise with LC3 (supplementary material Fig. S5) suggesting that these were indeed early autophagic structures. We also did not observe any colocalisation of the Atg5 structures with the Golgi markers p230 (supplementary material Fig. S6) (Derby et al., 2007) or golgin-84 (Satoh et al., 2003) and the Atg5 in these structures was not associated with the ER proteins BiP (Haas, 1994) or Grp94 (Argon and Simen, 1999) (data not shown). However, Rab5 associated with these Atg5-positive puncta, which is compatible with a role for Rab5 in early mammalian autophagy (Fig. 2g). We only observed very rare colocalisation of Atg5 and Atg12 in such puncta (Fig. 2h). It should be noted that these experiments were performed under constitutive autophagy conditions (full medium containing serum and amino acids) in cells with Rab5 inhibition. Rab5 inhibition or 3MA treatment was required to allow visualisation of sufficient numbers of these structures for characterisation. The accumulation of Atg5 structures by Vps34 or Rab5 inhibition might reflect a block in the progression of Atg5-positive membranes to the formation of autophagic vacuoles, which suggests a role of Rab5 in very early steps of autophagy. The observation that the Atg5 in these puncta was only rarely associated with Atg12 led to the hypothesis that defective Atg5-Atg12 conjugation is causally related to puncta formation.

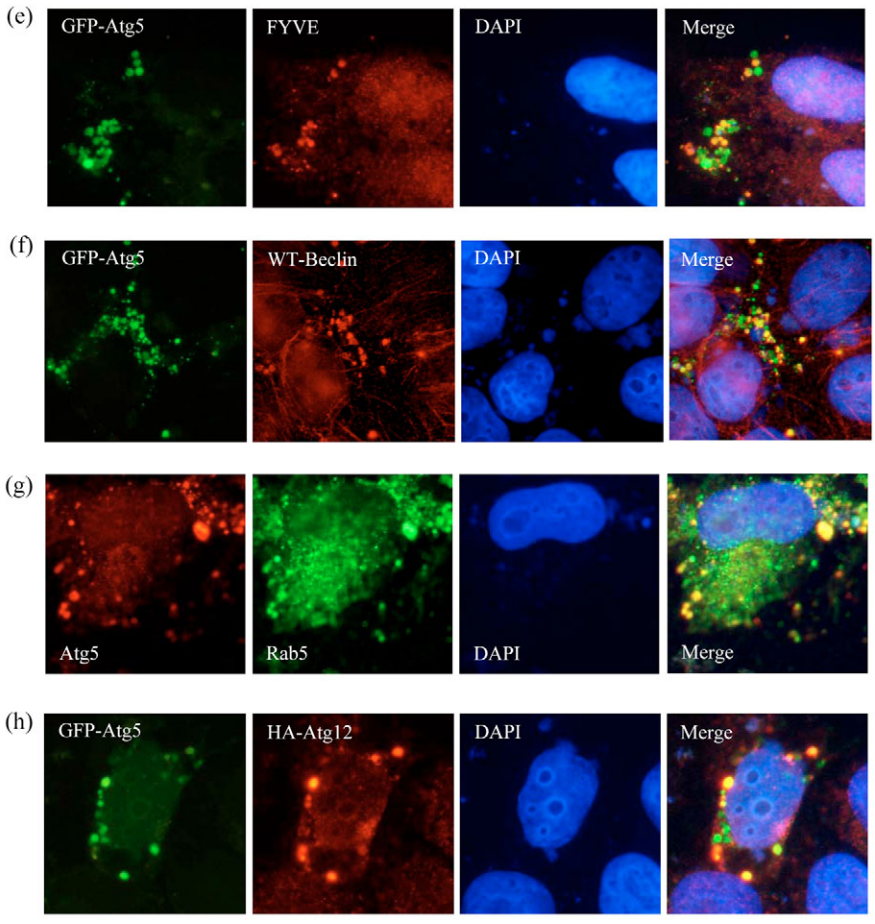

Fig. 2e-h. See previous page for legend.

Both Rab5 and Vps34 regulate Atg5-Atg12 conjugation

The possibility that defective Atg5-Atg12 conjugation leads to defective autophagosome formation associated with an accumulation of phagophores enriched in unconjugated Atg5 was compatible with the similarity of the above results and the phenotypes seen in apg7Δ or apg12Δ yeast strains, which typically show one to five large Atg5-positive punctate structures per cell, (a phenomenon that is very rare in wild-type cells) (George et al., 2000). Thus, when we knocked down Atg7 (an E1-like enzyme crucial for Atg5-Atg12 conjugation; supplementary material Fig. S7) in mammalian cells, we observed increased GFP-Atg5 structures, consistent with those observed in yeast (Fig. 3a). These Atg5-positive structures also colocalised with beclin 1 (supplementary material Fig. S8). Accordingly, we tested whether the increase in Atg5 structures seen with Rab5 or Vps34 inhibition was associated with aberrant Atg5-Atg12 conjugation. Consistent with this hypothesis and with the only very rare colocalisation of Atg12 and Atg5 in the puncta that accumulated following inhibition of Rab5 (Fig. 2h), we found that the ratio of Atg5-Atg12 complex formed compared with the pool of unconjugated Atg12 was significantly lower in cells expressing DN-Rab5 (Fig. 3b). 3MA treatment and siRNA knockdown of Vps34 also had similar effects on Atg5-Atg12 conjugation compared with those seen with

loss-of-function of Rab5 (DN-Rab5), a Vps34 activator (Fig. 3c, left and right respectively). We also found decreased levels of Atg5-Atg12 complex compared with free Atg12 when we knocked down all Rab5 isoforms simultaneously (Fig. 3d, left). This effect was similar to the conjugation defect we observed with Atg7 knockdown (Fig. 3d, right). Thus, Rab5 inhibition and loss of activity of Vps34

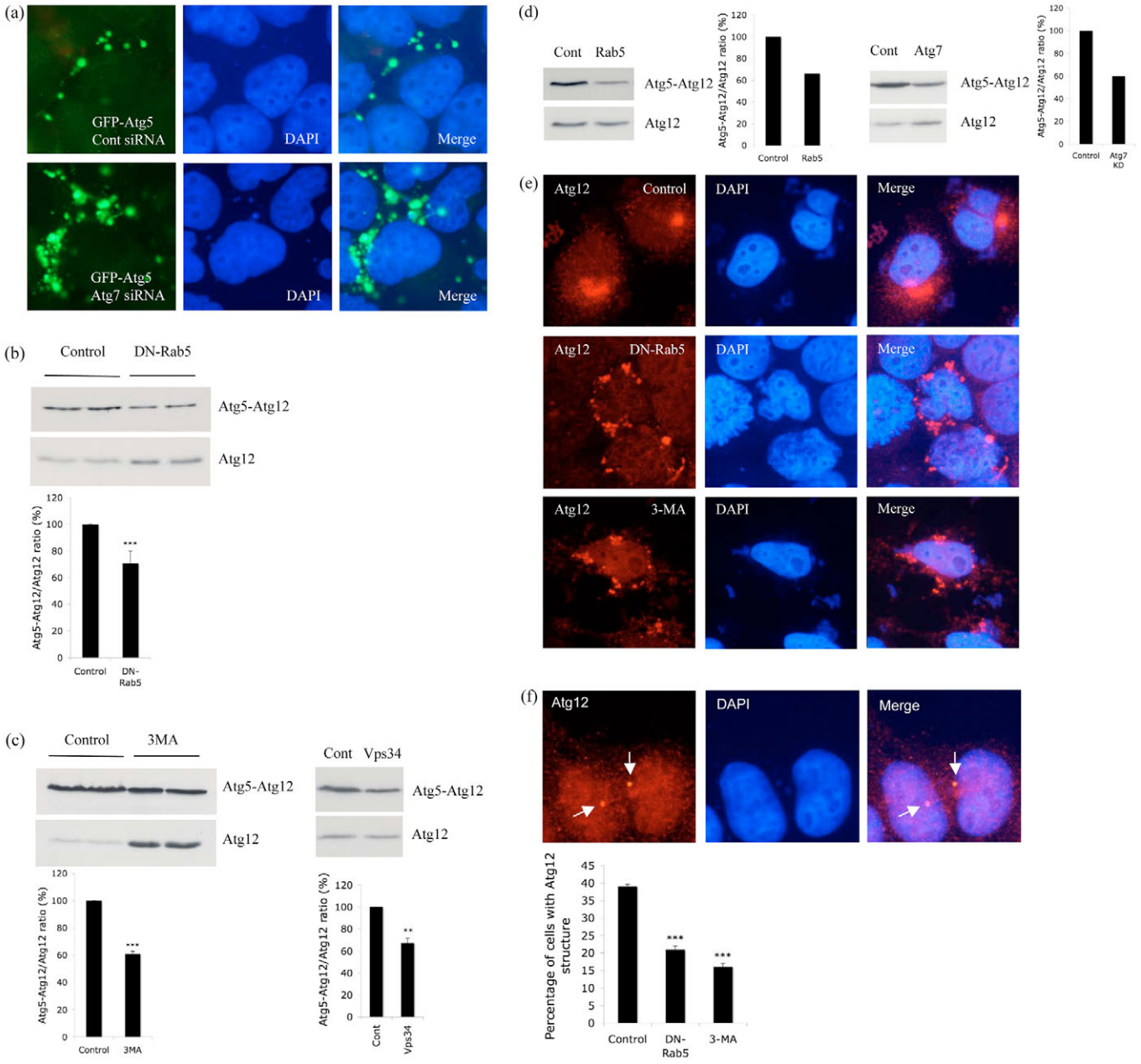

Fig. 3. Aberrant conjugation of Atg5 with Atg12 after Rab5 inhibition. (a) HeLa cells transfected with control or Atg7 siRNA for 48 hours were subjected to a second round of transfection with GFP-Atg5 together with the siRNA for another 24 hours. Then the cells were fixed following saponin extraction to visualise the GFP-Atg5 structures (green). (b) HeLa cells transfected with control vector or DN-Rab5 together with HA-Atg12 and Atg5 were subjected to western blot analysis with anti-HA antibody to detect free Atg12 and the Atg5-Atg12 complex. The ratio of Atg5-Atg12 versus free Atg12 is shown in the graph. Data are from four independent experiments; ***P<0.0001. (c) Atg5-Atg12:Atg12 ratio obtained from experiments similar to those shown in b, but performed in the presence or absence (control) of 3-methyladenine (3-MA; four independent experiments; left), or with control siRNA or siRNA targeting Vps34 (three independent experiments; right); ***P<0.0001, **P<0.001. (d) HeLa cells transfected simultaneously with siRNA targeting Rab5a, Rab5b and Rab5c (Rab5; left), Atg7 (right) or control siRNA for 48 hours were subjected to a second round of transfection with Atg5 and HA-Atg12 together with the Rab5 or Agt7 siRNA for another 24 hours. Western blot analysis was performed using anti-HA antibody to detect free Atg12 and the Atg5-Atg12 complex. Representative images from two independent, reproducible experiments are shown. (e) Immunostaining of HeLa cells transfected with either control (in the prescence or absence of 3-MA) or DN-Rab5 and HA-Atg12 for 24 hours after saponin extraction with anti-HA antibody (red). DAPI stained nuclei are in blue. (f) Immunostaining of HeLa cells transfected with control (with or without 3-MA) or DN-Rab5 for 24 hours after saponin extraction with anti-Atg12 antibody (red). DAPI stained nuclei are in blue. Arrows indicate punctate Atg12 structures in control cells. Quantification of cells with the punctate Atg12 structures in control, 3MA or DN-Rab5 in percent are given in the bar graph. ***P<0.0001.

(which is activated by Rab5) have a range of similar phenotypes: suppression of autophagy, increased numbers of Atg5-positive structures and decreased Atg5-Atg12 conjugation.

As both Rab5 and Vps34 are likely to regulate Atg5-Atg12 conjugation, which, in turn, regulates formation of autophagic vacuoles from Atg5-rich phagophores, we also looked at the distribution of Atg12 in saponin-extracted cells with Rab5 inhibition. In control cells, overexpressed Atg12 was located in a single large juxtanuclear domain (Fig. 3e), which did not change with the presence or absence of Atg5 overexpression (data not shown). However, with Rab5 inhibition, Atg12 was re-distributed to several peripheral small punctate structures (Fig. 3e), a phenomenon also seen with 3MA treatment (Fig. 3e). Similarly, when we looked at the distribution of endogenous Atg12, it was distributed in a single juxtanuclear domain (reminiscent of the yeast PAS) in wild-type cells (Fig. 3f). However, neither dominant-negative inhibition of Rab5 nor 3MA treatment significantly decreased the percentage of cells with these punctate endogenous Atg12 structures (Fig. 3f). The significance of the Atg12 re-distribution is still a matter of ongoing research, but leads to the hypothesis that Rab5 inhibition or 3MA treatment affects the accessibility of Atg12 for the conjugation process, probably by re-distributing it away from its normal cellular localisation. Alternatively, the decrease in Atg5-Atg12 conjugation that we observed with Rab5 inhibition or 3MA treatment might result in aberrant accumulation of unconjugated Atg12.

Rab5 is found in a macromolecular complex containing Vps34 and beclin 1

Since a macromolecular complex containing Vps34 and beclin 1 regulates the early nucleation step in autophagy, we next tested whether Rab5 was found in such a complex. We tested whether Rab5 interacted with beclin 1, because both proteins interact with Vps34 (Christoforidis et al., 1999; Kihara et al., 2001a), beclin 1 is associated with phagophores, and our data suggests that Rab5 acts at the autophagosome precursor stage and is also associated with such structures (Fig. 2g). In 3MA-treated cells, we observed colocalisation of endogenous Rab5 and beclin 1 (Fig. 4a), particularly in structures similar to those that accumulated when Rab5 or Vps34 were inhibited (e.g. Fig. 2). These putative autophagosome-precursors are precisely where we expected such colocalisation to occur. We also found strong colocalisation of beclin 1 with an activated Rab5 mutant (Fig. 4b). We used activated Rab5 because this forms large clear vesicles that allow unambiguous visualisation of membrane colocalisation of Rab5 with other proteins, a strategy frequently used for Rab5-interactor immunocytochemistry studies (Shin et al., 2005). We next looked for interaction of endogenous Rab5 with beclin 1 by immunoprecipitation. Rab5 interacted with beclin 1 (immunoprecipitated for beclin 1 and detected for Rab5) only in the presence of Vps34 suggesting that Rab5 is part of the macromolecular complex containing beclin 1 and Vps34 (Fig. 4c). Indeed, beclin 1 knockdown (supplementary material Fig. S9) enhances mutant huntingtin (Q74) aggregation (Fig. 4d) (Shibata et al., 2006), which is compatible with the knowledge that this will impair autophagosome formation. Crucially, beclin 1 knockdown led to decreased Atg5-Atg12 conjugation (Fig. 4e), which is compatible with the concept that both beclin 1 and Rab5 activity are required for Vps34 function in autophagosome formation. Thus, Rab5 activation of Vps34 probably regulates

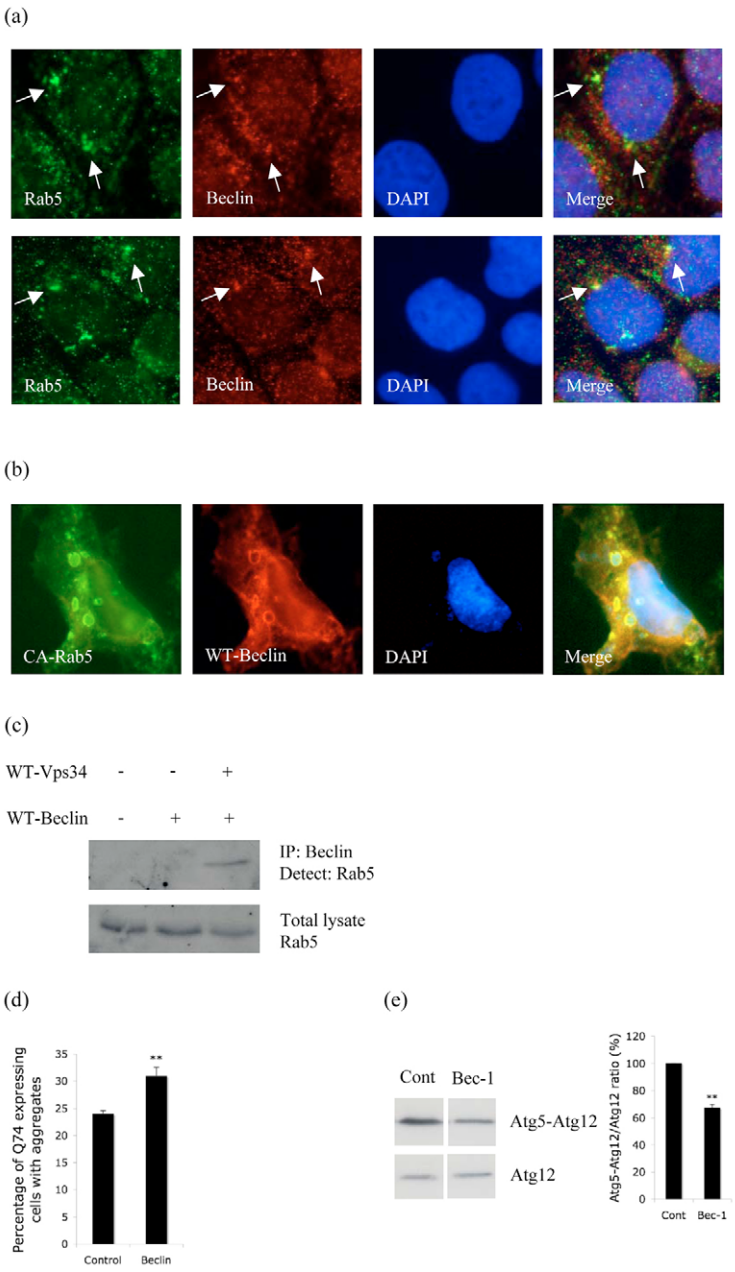

Fig. 4. Rab5 is part of a macromolecular complex containing Vps34 and beclin 1. (a) Colocalisation of endogenous Rab5 (green) and endogenous beclin 1 (red) in 3MA-treated HeLa cells after saponin extraction. DAPI-stained nuclei are in blue. (b) Colocalisation of constitutive active Rab5 (CA-Rab5; green) with wild-type beclin 1 (WT-Beclin, red). (c) COS-7 cells transfected with control vector alone (lane 1) or Flag-tagged wild-type beclin 1 alone (lane 2) or wild-type beclin 1 with wild-type Vps34 (lane 3) were immunoprecipitated using anti-Flag antibody (to immunoprecipitate beclin 1) and blotted for Rab5 using an anti-Rab5 antibody. (d) Q74-HA aggregation in HeLa cells transfected with control siRNA or siRNA targeting beclin 1 as described in Fig. 2d; $P<0.005$. (e) Ratio of Atg5-Atg12 conjugate to Atg12 (data from three independent experiments) in HeLa cells transfected with control siRNA or siRNA targeting beclin 1 for 72 hours. Atg5 and HA-Atg12 were transfected for the last 24 hours. $P=0.0003$.

not only endosome maturation and multivesicular body formation but also, through recruitment of beclin 1, initiation of autophagic vacuole formation.

The effect of Rab5 on autophagy is not due to a general inhibition of the endocytic pathway

Since Rab5 is an important regulator of the endocytic pathway, we further tested whether the effects we saw with Rab5 inhibition are indirect consequences of endocytosis inhibition. We first perturbed the function of dynamin, a large GTPase essential for clathrin-mediated endocytosis, using dominant-negative dynamin (DN-Dyn). DN-Dyn increased the percentage of COS-7 cells with aggregates and cell death similar to DN-Rab5 (Fig. 5a). However, unlike Rab5, overexpression of DN-Dyn increased the size and also the number of LC3-positive autophagic vacuoles (Fig. 5b-d) similar to what we and others observe after treatment with BafA1 (Bampton et al., 2005). This suggests that DN-Dyn inhibits autophagy at the level of autophagic-lysosomal delivery similar to BafA1. Accordingly, we found decreased colocalisation of LC3-labelled vesicles with the lysosomal marker lgp120, similar to colocalisation observed in cells treated with BafA1 (Fig. 5e). Previous studies have shown that autophagosomes may fuse with endosomes to form intermediary compartments called amphisomes, which subsequently fuse with lysosomes (Berg et al., 1998). Thus, it is possible that inhibition of the endocytic flux prevents the formation of amphisomes, thereby also inhibiting a subsequent step in the autophagic pathway, amphisome-lysosome fusion. Again, unlike Rab5, we did not see any increase in the Atg5 structures (supplementary material Fig. S10) nor could we observe any change in the ratio of Atg5-Atg12 complex to free Atg12 when dynamin was inhibited (Fig. 5f).

These results suggest that DN-Dyn inhibits autophagy at the level of autophagic-lysosomal delivery, which is similar to what has been previously reported using Vps4, an AAA ATPase involved in trafficking through the endocytic pathway (Nara et al., 2002). Overexpression of dominant-negative Vps4 showed defects in autophagy-dependent bulk protein degradation due to an impairment

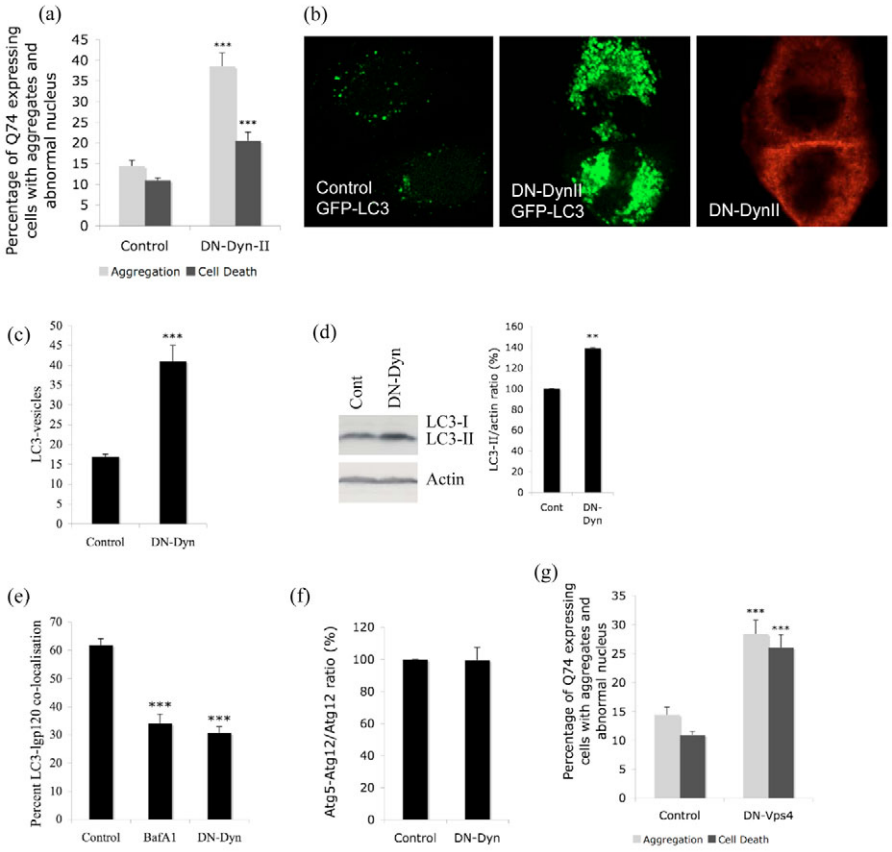

Fig. 5. (a) Quantification of GFP-expressing COS-7 cells with aggregates and abnormal nuclear morphology transiently transfected with dominant-negative dynamin II (DN-Dyn-II) or empty vector control and EGFP-tagged huntingtin exon 1 containing 74 polyglutamine repeats (3:1 ratio) for 48 hours. ***P<0.0001. (b) Distribution of GFP-LC3 vesicles in control (left) or DN-dynamin (red) transfected cells (right). (c) COS-7 cells were transiently transfected with empty vector (Control), DN-dynamin (DN-Dyn) and GFP-LC3 (3:1 ratio) for 24 hours. GFP-positive cells with an increased number of LC3-positive vesicles (>20 vesicles per cell) were quantified; ***P<0.0001. (d) Lysates from HeLa cells expressing empty vector control (Cont) or DN-dynamin (DN-Dyn) were blotted for endogenous LC3, and actin as control. Quantification of band intensities from four independent experiments is shown; **P<0.001. Under exposure conditions that allow endogenous LC3-II quantification in these cells, the LC3-I signal is frequently too low to be detected. (e) NRK cells were transiently transfected for 15 hours with either empty vector [control; with or without bafilomycin A1 (BafA1)] or DN-dynamin (DN-Dyn), and mRFP-LC3 and GFP-lgp120. mRFP-LC3 and GFP-lgp120 double-stained vesicles in individual cells are given in percent (Jahreiss et al., 2008). ***P<0.0001. (f) HeLa cells transfected with control vector or DN-dynamin (DN-Dyn) together with HA-Atg12 and Atg5 were subjected to western blot analysis using anti-HA antibody to detect free Atg12 and the Atg5-Atg12 complex. Atg5-Atg12:Atg12 ratio from three independent experiments is shown. (g) Quantification of GFP-expressing COS-7 cells with aggregates and abnormal nuclear morphology transiently transfected with dominant-negative (DN) Vps4 or empty vector control and EGFP-tagged huntingtin exon 1 containing 74 polyglutamine repeats (3:1 ratio) for 48 hours. ***P<0.0001.

in the formation of autolysosomes (Nara et al., 2002). Similar to our results for DN-Dyn we did not see an increase in Atg5 structures (data not shown) or decrease in the levels of the Atg5-Atg12 complex with DN-Vps4 (supplementary material Fig. S11) but, similar to experiments using DN-Dyn (Fig. 5a) or BafA1 (Ravikumar et al., 2002), we observed an increase in the aggregation and associated cell death of huntingtin Q74 in the presence of DN-Vps4 (Fig. 5g).

Results obtained using DN-Dyn were identical to those when using siRNA targeting clathrin heavy chain (supplementary material Fig. S12), which is involved in formation of clathrin-coated vesicles. siRNA targeting clathrin heavy chain increased the percentage of HeLa cells with aggregates (Fig. 6a), increased the number and size of LC3-labelled autophagic vacuoles (Fig. 6b,c), did not increase the number of Atg5 structures (data not shown) and had no effect on Atg5-Atg12 conjugation (Fig. 6d). Finally, we also looked at the effect of the endocytosis inhibitor methyl-β-cyclodextrin (β-CD) on LC3-II levels both in the presence or absence of BafA1 (supplementary material Fig. S13). β-CD increased the levels of LC3-II in the absence of BafA1, but had no effect when BafA1 was present (Fig. 6e); which again suggests that inhibition of endocytosis blocks autophagic-lysosomal delivery. DN-Dyn and siRNA targeting clathrin heavy chain both had similar effects on LC3-II levels in the presence of BafA1 similar to β-CD (supplementary material Figs S14, S15). Thus, Rab5 inhibition, which impairs Atg5-Atg12 conjugation, autophagosome (and

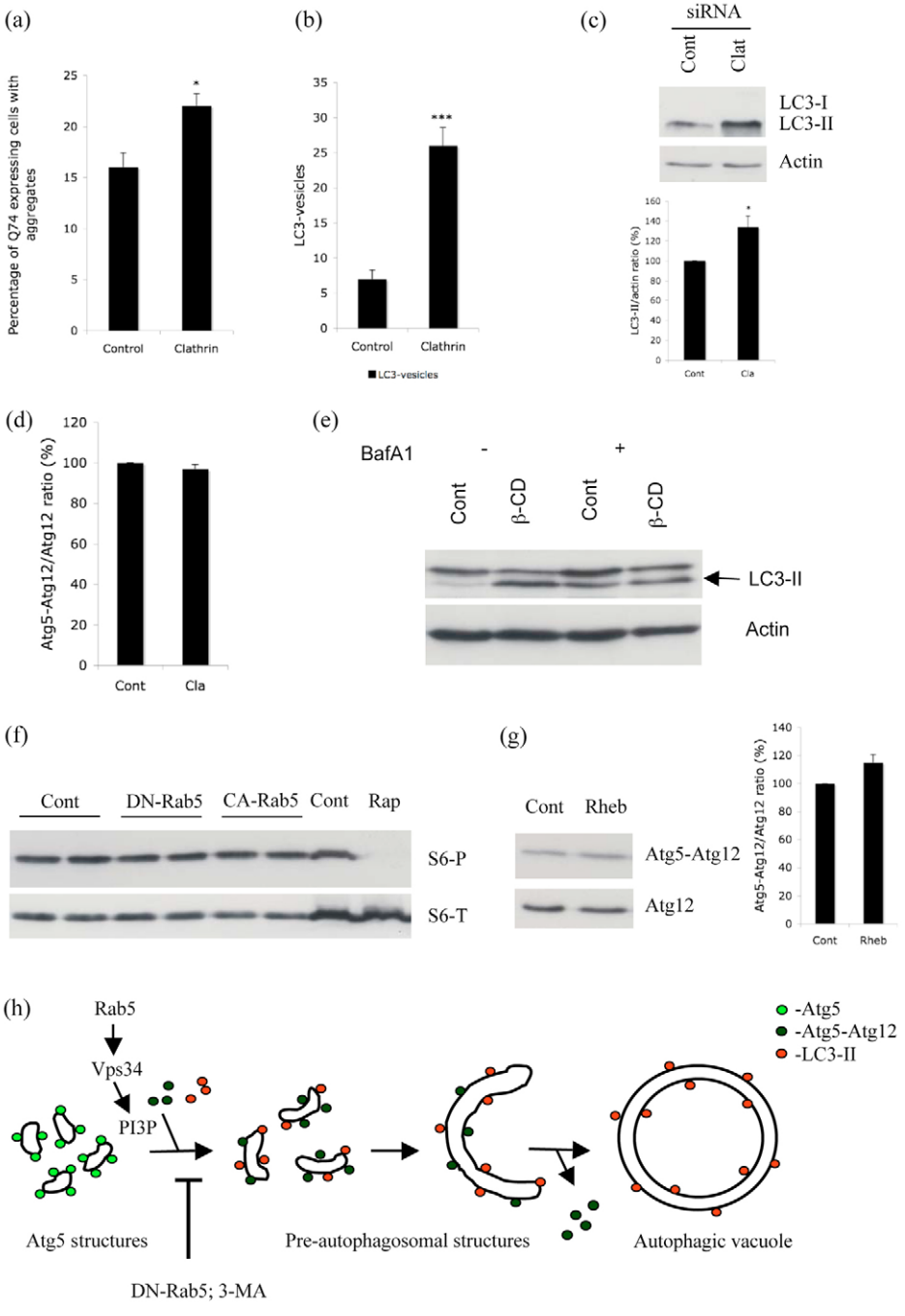

Fig. 6. (a) HeLa cells transfected with control siRNA or siRNA targeting clathrin heavy chain for 48 hours were subsequently transfected with EGFP-tagged huntingtin exon 1 containing 74 polyglutamine repeats (Q74) for 24 hours. Quantification of Q74 expressing cells with aggregates is shown in the graph. *P<0.01. (b) HeLa cells stably expressing GFP-LC3 were transfected with control or clathrin siRNA for 72 hours, numbers of LC3-positive vesicles were counted (>20 vesicles per cell); ***P<0.0001. (c) HeLa cells transfected with control siRNA or siRNA targeting clathrin heavy chain for 72 hours were subjected to western blot analysis using anti-LC3 and anti-actin antibodies. Under exposure conditions that allowed endogenous LC3-II quantification in these cells, the LC3-I signal was frequently too low to be detected. Quantification of band intensities from three independent experiments is shown. *P<0.05. (d) HeLa cells transfected with control siRNA (Cont) or siRNA targeting clathrin heavy chain (Cla) for 48 hours were subsequently transfected with HA-Atg12 and Atg5 for a further 24 hours. Western blot analysis was performed with anti-HA antibody to detect free Atg12 and the Atg5-Atg12 complex. The Atg5-Atg12:Atg12 ratio from three independent experiments is shown. (e) HeLa cells stably expressing GFP-LC3 were left untreated (Cont) or treated with 5 mM methyl-β-cyclodextrin (β-CD), in the presence (+) or absence (–) of bafilomycin A1 (BafA1) for 6 hours were subjected to western blot analysis using anti-GFP (to detect LC3) and anti-actin antibodies. (f) Lysates from HeLa cells transfected with empty vector (Cont), DN-Rab5 or CA-Rab5 were blotted for phosphorylated (S6-P) and total (S6-T) ribosomal protein S6. Lysate from cells treated with rapamycin (Rap) was used as a positive control. (g) HeLa cells transfected with control vector (Cont) or wild-type Rheb together with HA-Atg12 and Atg5 were subjected to western blot analysis with anti-HA antibody to detect free Atg12 and the Atg5-Atg12 complex. The Atg5-Atg12:Atg12 ratio from three independent experiments is shown. (h) Schematic hypothetical representation of how autophagy is regulated by Rab5. Our data suggest that the Atg5 structures are probably precursors of the pre-autophagosomal structures. The accumulation of Atg5 structures that were observed by us following inhibition of Rab5 or Vps34 might be owing to a block in the progression from early Atg5-positive autophagosomal structures to the formation of autophagic vacuoles.

LC3-II) formation, and which is associated with an accumulation of Atg5-positive structures, has different effects to a range of endocytosis inhibitors (such as β-CD, DN-Dyn, DN-Vps4 or siRNA targeting clathrin) that do not affect Atg5-Atg12 conjugation but block autophagic-lysosomal delivery and increase LC3-II levels. (The specificity of the effect of Rab5 inhibition versus endocytosis inhibition on LC3-II levels has been clearly demonstrated in our experiments where we have treated cells with BafA1.) This argues that the effect on autophagosome formation owing to the loss of Rab5 function is not due to effects on endocytosis.

Rab5 effect on autophagy is not due to mTOR signalling

Previous studies in *Drosophila* have shown that disruption of endocytosis can lead to changes in the target of rapamycin (TOR) signalling, a key process regulating autophagy (Hennig et al., 2006). Since Rab5 regulates endocytosis, we tested whether the conditions of Rab5 inhibition or activation alters the mTOR-signalling pathway. mTOR directly phosphorylates at least two effectors: S6 kinase-1 and 4EBP1. S6 kinase-1 phosphorylates the ribosomal protein S6. The levels of phosphorylation of any of these downstream targets are recognised indicators of mTOR activity in the cell (Jacinto and Hall, 2003). Accordingly, we tested whether DN-Rab5 or CA-Rab5 altered the mTOR pathway by looking at the phosphorylation levels of S6. We did not observe any changes in the phosphorylation of S6 (Fig. 6f). We also did not see any changes in the phosphorylation levels of S6 kinase-1 or 4EBP1 using DN-Rab5 or CA-Rab5 (data not shown). Thus, the effects we observed with Rab5 were not owing to alterations in the mTOR signalling. Furthermore, when mTOR signaling was activated by overexpressing Ras homolog enriched in brain (Rheb; see supplementary material Fig. S16) we did not observe the same effects we observed when expressing DN-Rab5; we did not detect an increase in Atg5 structures (data not shown) and did not see any decrease in the Atg5-Atg12 conjugate compared with the pool of unbound Atg12 (Fig. 6g). Taken together, our results suggest that the role of Rab5 on autophagy is independent of its effects on endocytosis and is not because of perturbations in mTOR signalling.

Conclusion

In conclusion, we show that Rab5 can modify the toxicity of polyglutamine in cell and fly models. These modifying effects are due to Rab5 regulating autophagy-dependent clearance of the toxic huntingtin mutant protein. Our data suggest that Rab5, previously considered as a specific endosome marker, also influences mammalian autophagy. Inhibition of Rab5 resulted in a decrease in LC3-positive vesicles suggesting a defect in the formation of autophagic vacuoles. Rab5 is an activator of Vps34, a PI 3-kinase essential for autophagy initiation, and we have shown that Rab5 is a new member of a complex that contains Vps34 and beclin 1, and that is associated with autophagosome precursors. Thus, the most parsimonious explanation of our data is that Rab5 acts as an activator for Vps34 in autophagy as it is known to do in endocytosis. This hypothesis is consistent with the various similarities we observed in cells expressing loss-of-function of Rab5 or Vps34. Loss of either enzyme activity decreased Atg5-Atg12 conjugation, a crucial step in early phagophore elongation. We speculate that accumulation of Atg5 structures concomitantly with Rab5 or Vps34 inhibition is owing to a block in their progression from early Atg5-positive autophagosomal structures to the formation of autophagosomes (Fig. 6h). This block might be due to a defect in Atg12 recruitment. Indeed, decreasing Atg5 conjugation (which is known to block autophagosome formation) also resulted in increased numbers of Atg5-positive autophagosome precursors.

Our data do not exclude the possibility that membranes for autophagosome biogenesis are derived from endosomes. However, the effect of Rab5 inactivation on Atg5-Atg12 conjugation and autophagosome synthesis is not seen when using a wide range of molecules that inhibit endocytosis (β-CD, DN-Dyn, DN-Vps4 and siRNA targeting clathrin) that instead impede autophagic flux by inhibiting autophagosome-lysosome fusion directly or by inhibiting the autophagosome-endosome fusion step. This suggests that inhibition of endocytosis through different mechanisms will also enhance aggregation and toxicity of polyglutamine by blocking autophagy. It is possible that the loss of Rab5 activity has effects on autophagy by perturbing other unrelated or unknown membrane trafficking pathways (distinct from endocytosis). However, it is important to point out that overexpression of CA-Rab5 or WT-Rab5 enhanced autophagosome synthesis and suppressed aggregation and toxicity of mutant huntingtin in tissue culture cells and in vivo.

We believe that our data suggest a sequential model in mammalian cells, in which PtdIns(3)*P* generated by Vps34, in a complex that comprises at least beclin 1 and active Rab5, is a key regulator of Atg12 conjugation to Atg5, a rate-limiting step in the conversion of Atg5-positive autophagosome precursors to Atg5-negative autophagosomes. On the one hand, inhibition of this putative cascade at a number of points will lead to impaired autophagy and enhance polyglutamine toxicity. On the other hand, better understanding of the initial rate-limiting steps of autophagy may provide opportunities for the rational design of more specific and safer autophagy-inducing therapeutic drugs than rapamycin (which affects many pathways). This may be of relevance to HD and also to a range of related neurodegenerative diseases caused by intracytosolic aggregate-prone proteins.

Materials and Methods

Mammalian cell culture and transfection

COS-7 and HeLa cells were grown in Dulbecco's modified Eagle's medium (DMEM) (Sigma) supplemented with 10% foetal bovine serum (FBS) (Sigma), 100 U/ml penicillin/streptomycin (Sigma), 2 mM L-glutamine (Sigma) at 37°C, 5% CO_2. DNA transfections were performed using lipofectamine reagent (Invitrogen). 20 nmol of control (cat. no. 4611), Atg7 (ID 135756), Rab5a (ID 120372), Rab5b (ID 120273), Rab5c (ID 120809), clathrin heavy chain (ID 107565), Vps34 (ID 143802) or beclin (ID 137200) siRNA (all from Ambion) were transfected using lipofectamine 2000 according to manufacturer's instructions.

Western blot analysis

Western blot analysis was carried out applying standard techniques using the ECL detection kit (Amersham). The primary antibodies used include anti-GFP (Clontech), anti-HA (Covance), anti-Myc and anti-actin (Sigma), anti-Atg7 (Rockland Inc.), anti-Atg5 and anti-Rab5 (Abcam), anti-Vps34 (Zymed) and anti-beclin (Cell Signaling technology). Densitometry analysis was performed using Image J 1.36b or Scion Image Beta 4.02 softwares. For immunoprecipitation, cells were suspended in lysis buffer (50 mM Tris HCl pH 7.4, 150 mM NaCl, 1 mM EDTA and 1% Triton X-100) for 30 minutes on ice and supernatants were removed by centrifugation at 13,000 rpm in a tabletop centrifuge for 7 minutes at 4°C. 30 µl of anti-M2 affinity gel (Sigma) was added to the sample and incubated at 4°C for 2 hours with gentle rocking. After incubation, tubes were spun for 30 seconds at 4°C at less than 4000 ***g***. Pellets were washed four times with 1 ml of chilled buffer A (20 mM Tris HCl pH 7.2, 2 mM $MgCl_2$,150 mM NaCl, 0.5% Nonidet P-40). Bound protein was eluted with 100 µl of 150 ng/µl 3×FLAG peptide in TBS.

Immunocytochemistry

Immunocytochemistry was performed in HeLa cells transfected with GFP-Atg5, extracted using 0.02% saponin and fixed using 4% paraformaldehyde. Saponin was prepared using PHEM buffer (60 mM NaPIPES, 25 mM NaHEPES, 10 mM EGTA 2 mM $MgCl_2$, pH 6.9) supplemented with 0.19 M NaCl. Primary antibodies used were anti-Myc, anti-Flag (Sigma), anti-Rab5 and anti-HA. Relevant negative controls without primary antibodies were performed alongside all experiments. Nuclei were stained with 4′6-diamidino-2-phenylindole (DAPI, 3 mg/ml; Sigma). Images were acquired

using a Nikon Digital Camera DXM1200 and a Nikon Eclipse E600 fluorescence microscope. We used Nikon ACT-1 version 2.12 acquisition software. Adobe Photoshop 6.0 (Adobe Systems, Inc.) was used for subsequent image processing.

Quantification of aggregate formation, abnormal nuclear morphologies, LC3-positive vesicles

Aggregate formation and nuclear morphology were assessed using a fluorescence microscope. An example of cells expressing the mutant huntingtin with 74 polyQ repeats (Q74) with aggregates (arrows) and an aggregate-containing cell with abnormal nuclear morphology (arrowhead) is shown in supplementary material Fig. S17. Two-hundred Q74-transfected COS-7 cells or MEFs were selected and the number of cells with aggregates are counted. The identity of the slides was unavailable to the observer until all slides had been studied. The experiments were performed in triplicate and repeated twice. Cells were considered dead if the DAPI-stained nuclei showed apoptotic morphology (fragmentation or pyknosis). Pyknotic nuclei are typically <50% the diameter of normal nuclei and show obvious and increased DAPI intensity. An example of cells with abnormal nuclear morphologies (arrows) is shown in supplementary material Fig. S18. For quantification of LC3, 100 EGFP- or mRFP-positive COS-7 cells were selected and cells with ~20 or more LC3-labelled vesicles were counted. The identity of the slides was unavailable to the observer until all slides had been studied. Examples of cells with (a) <20 vesicles and (b) >20 vesicles are shown in supplementary material Fig. S19.

Endocytosis assay

HeLa cells were pre-treated with or without 5 mM methyl-β-cyclodextrin (β-CD) for 24 hours. Cells were washed with serum-free medium containing 0.5% BSA and then incubated at 4°C with 10 μg/ml Alexa-Fluor-594-labeled human transferrin (Molecular Probes) for 30 minutes. Excess label was washed off, after which the cells were incubated at 37°C for 10 minutes to allow uptake of the ligand in serum-free medium containing 0.5% BSA with or without 5 mM β-CD. Cells were then fixed with 4% paraformaldehyde in 0.1 M PBS pH 7.6. Images were acquired on a Zeiss LSM510 META confocal microscope (63×1.4NA plan-apochromat oil immersion lens) at room temperature using Zeiss LSM510 v3.2 software (Carl Zeiss, Inc.).

Drosophila strains

Recombinant males of genotype *w; CyO/If; UAS-Rab5-EGFP elavGal4/MKRS,* carrying Rab5-EGFP (Wucherpfennig et al., 2003) and elav-Gal4 3A4 (Luo et al., 1994) on the third chromosome (gift of V. Korolchuk, Department of Genetics, University of Cambridge, UK) were crossed with *y w; gmr-Htt(exon1)Q120* (Jackson et al., 1998) virgins. As a control both *y w; gmr-Htt(exon1)Q120* and *w; CyO/If; UAS-Rab5-EGFP-elavGal4/MKRS* virgins were crossed with an isogenic w^{1118} line (Ryder et al., 2004). Rhabdomeres were scored using the pseudopupil technique as previously described (Franceschini and Kirschfeld, 1971). Means, standard errors and statistical comparisons using a *t*-test wer calculated from six independent experiments. In each experiment we evaluated ten eyes per genotype, and 15 ommatidia per eye.

Statistics

Pooled estimates for the changes in aggregate formation or cell death resulting from perturbations assessed in multiple experiments, were calculated as odds ratios with 95% confidence intervals. We have used this method frequently in the past to allow analysis of data from multiple independent experiments (Wyttenbach et al., 2001). Odds ratios and *P* values were determined using unconditional logistical regression analysis and the general log-linear analysis option of SPSS 9 software. 95% confidence limits for the odds ratio were obtained by using the robust variance approach. Significance levels for comparisons between groups were determined with *t* tests, where appropriate, for parametric data and with Mann-Whitney *U* tests for non-parametric data, using the STATVIEW software, version 4.53 (Abacus Concepts, Berkeley, CA).

We are grateful to G. Jackson (UCLA, CA) for HD flies; M. González-Gáitan (Max Planck Institute of Molecular Cell Biology and Genetics, Dresden, Germany) for UAS-EGFP-Rab5 flies; V. Korolchuk (CIMR, UK) for the Rab5 recombinants that we have used in this paper; T. Yoshimori (National Institute of Genetics, Mishima, Japan) for GFP-LC3 and Myc-LC3; A. Tolkovsky (Department of Biochemistry, Cambridge University, UK) for GFP-LC3 stable HeLa cells; K. L. Guan (University of Michigan, Ann Arbor, MI) for Rheb; B. Beaumelle (University of Montpellier II, France) for WT-, S34N-Rab5 and K44A Dynamin; J. P. Luzio (CIMR, UK) for Vps34; M. Robinson (CIMR, UK) for Alex Fluor 594-labeled human transferrin; B. Levine (UT Southwestern, Dallas, TX) for beclin 1, H. Stenmark (The Norwegian Radium Hospital, Oslo, Norway) for myc-FYVE; N. Mizushima (The Tokyo Metropolitan Institute of Medical Science, Japan) for HA-Atg12 and Atg5; $Atg5^{-/-}$ and WT-MEF cells; A. Sorkin (University of Colorado Health Sciences Center, Denver, CO) for N34S and Q79L Rab5; J. Stankova (University of Sherbrooke, Québec, Canada) for K44A Dynamin; X. Wang (The University of Utah, Salt Lake City, UT) for DN-Vps4B; Eléonore Mayola for technical support. We are grateful for MRC (D.C.R. and C.O'K.); EU Framework VI (EUROSCA) (D.C.R.) funding; D.C.R. is a Wellcome Trust Senior Clinical Fellow.

References

Argon, Y. and Simen, B. B. (1999). GRP94, an ER chaperone with protein and peptide binding properties. *Semin. Cell Dev. Biol.* **10**, 495-505.

Arrasate, M., Mitra, S., Schweitzer, E. S., Segal, M. R. and Finkbeiner, S. (2004). Inclusion body formation reduces levels of mutant huntingtin and the risk of neuronal death. *Nature* **431**, 805-810.

Bampton, E. T., Goemans, C. G., Niranjan, D., Mizushima, N. and Tolkovsky, A. M. (2005). The dynamics of autophagy visualized in live cells: from autophagosome formation to fusion with endo/lysosomes. *Autophagy* **1**, 23-36.

Berg, T. O., Fengsrud, M., Strømhaug, P. E., Berg, T. and Seglen, P. O. (1998). Isolation and characterization of rat liver amphisomes. Evidence for fusion of autophagosomes with both early and late endosomes. *J. Biol. Chem.* **273**, 21883-21892.

Berger, Z., Ravikumar, B., Menzies, F. M., Oroz, L. G., Underwood, B. R., Pangalos, M. N., Schmitt, I., Wullner, U., Evert, B. O., O'Kane, C. J. et al. (2006). Rapamycin alleviates toxicity of different aggregate-prone proteins. *Hum. Mol. Genet.* **15**, 433-442.

Blommaart, E. F., Krause, U., Schellens, J. P., Vreeling-Sindelarova, H. and Meijer, A. J. (1997). The phosphatidylinositol 3-kinase inhibitors wortmannin and LY294002 inhibit autophagy in isolated rat hepatocytes. *Eur. J. Biochem.* **243**, 240-246.

Bucci, C., Parton, R. G., Mather, I. H., Stunnenberg, H., Simons, K., Hoflack, B. and Zerial, M. (1992). The small GTPase rab5 functions as a regulatory factor in the early endocytic pathway. *Cell* **70**, 715-728.

Christoforidis, S., Miaczynska, M., Ashman, K., Wilm, M., Zhao, L., Yip, S. C., Waterfield, M. D., Backer, J. M. and Zerial, M. (1999). Phosphatidylinositol-3-OH kinases are Rab5 effectors. *Nat. Cell Biol.* **1**, 249-252.

Derby, M. C., Lieu, Z. Z., Brown, D., Stow, J. L., Goud, B. and Gleeson, P. A. (2007). The trans-Golgi network golgin, GCC185, is required for endosome-to-Golgi transport and maintenance of Golgi structure. *Traffic* **8**, 758-773.

Franceschini, N. and Kirschfeld, K. (1971). [Pseudopupil phenomena in the compound eye of drosophila]. *Kybernetik* **9**, 159-182.

Gaullier, J. M., Simonsen, A., D'Arrigo, A., Bremnes, B., Stenmark, H. and Aasland, R. (1998). FYVE fingers bind PtdIns(3)P. *Nature* **394**, 432-433.

George, M. D., Baba, M., Scott, S. V., Mizushima, N., Garrison, B. S., Ohsumi, Y. and Klionsky, D. J. (2000). Apg5p functions in the sequestration step in the cytoplasm-to-vacuole targeting and macroautophagy pathways. *Mol. Biol. Cell* **11**, 969-982.

Haas, I. G. (1994). BiP (GRP78), an essential hsp70 resident protein in the endoplasmic reticulum. *Experientia* **50**, 1012-1020.

Hara, T., Nakamura, K., Matsui, M., Yamamoto, A., Nakahara, Y., Suzuki-Migishima, R., Yokoyama, M., Mishima, K., Saito, I., Okano, H. et al. (2006). Suppression of basal autophagy in neural cells causes neurodegenerative disease in mice. *Nature* **441**, 885-889.

Hennig, K. M., Colombani, J. and Neufeld, T. P. (2006). TOR coordinates bulk and targeted endocytosis in the Drosophila melanogaster fat body to regulate cell growth. *J. Cell Biol.* **173**, 963-974.

Jacinto, E. and Hall, M. N. (2003). Tor signalling in bugs, brain and brawn. *Nat. Rev. Mol. Cell Biol.* **4**, 117-126.

Jackson, G. R., Salecker, I., Dong, X., Yao, X., Arnheim, N., Faber, P. W., MacDonald, M. E. and Zipursky, S. L. (1998). Polyglutamine-expanded human huntingtin transgenes induce degeneration of Drosophila photoreceptor neurons. *Neuron* **21**, 633-642.

Jahreiss, L., Menzies, F. M. and Rubinsztein, D. C. (2008). The itinerary of autophagosomes: from peripheral formation to kiss-and-run fusion with lysosomes. *Traffic* **9**, 574-587.

Kabeya, Y., Mizushima, N., Ueno, T., Yamamoto, A., Kirisako, T., Noda, T., Kominami, E., Ohsumi, Y. and Yoshimori, T. (2000). LC3, a mammalian homologue of yeast Apg8p, is localized in autophagosome membranes after processing. *EMBO J.* **19**, 5720-5728.

Kihara, A., Kabeya, Y., Ohsumi, Y. and Yoshimori, T. (2001a). Beclin-phosphatidylinositol 3-kinase complex functions at the trans-Golgi network. *EMBO Rep.* **2**, 330-335.

Kihara, A., Noda, T., Ishihara, N. and Ohsumi, Y. (2001b). Two distinct Vps34 phosphatidylinositol 3-kinase complexes function in autophagy and carboxypeptidase Y sorting in Saccharomyces cerevisiae. *J. Cell Biol.* **152**, 519-530.

Klionsky, D. J. and Ohsumi, Y. (1999). Vacuolar import of proteins and organelles from the cytoplasm. *Annu. Rev. Cell Dev. Biol.* **15**, 1-32.

Komatsu, M., Waguri, S., Chiba, T., Murata, S., Iwata, J., Tanida, I., Ueno, T., Koike, M., Uchiyama, Y., Kominami, E. et al. (2006). Loss of autophagy in the central nervous system causes neurodegeneration in mice. *Nature* **441**, 880-884.

Kovacs, A. L., Gordon, P. B., Grotterod, E. M. and Seglen, P. O. (1998). Inhibition of hepatocytic autophagy by adenosine, adenosine analogs and AMP. *Biol. Chem.* **379**, 1341-1347.

Lunkes, A., Lindenberg, K. S., Ben-Haiem, L., Weber, C., Devys, D., Landwehrmeyer, G. B., Mandel, J. L. and Trottier, Y. (2002). Proteases acting on mutant huntingtin

generate cleaved products that differentially build up cytoplasmic and nuclear inclusions. *Mol. Cell* **10**, 259-269.

Luo, L., Liao, Y. J., Jan, L. Y. and Jan, Y. N. (1994). Distinct morphogenetic functions of similar small GTPases: Drosophila Drac1 is involved in axonal outgrowth and myoblast fusion. *Genes Dev.* **8**, 1787-1802.

Mizushima, N., Yamamoto, A., Hatano, M., Kobayashi, Y., Kabeya, Y., Suzuki, K., Tokuhisa, T., Ohsumi, Y. and Yoshimori, T. (2001). Dissection of autophagosome formation using Apg5-deficient mouse embryonic stem cells. *J. Cell Biol.* **152**, 657-668.

Nara, A., Mizushima, N., Yamamoto, A., Kabeya, Y., Ohsumi, Y. and Yoshimori, T. (2002). SKD1 AAA ATPase-dependent endosomal transport is involved in autolysosome formation. *Cell Struct. Funct.* **27**, 29-37.

Narain, Y., Wyttenbach, A., Rankin, J., Furlong, R. A. and Rubinsztein, D. C. (1999). A molecular investigation of true dominance in Huntington's disease. *J. Med. Genet.* **36**, 739-746.

Pal, A., Severin, F., Lommer, B., Shevchenko, A. and Zerial, M. (2006). Huntingtin-HAP40 complex is a novel Rab5 effector that regulates early endosome motility and is up-regulated in Huntington's disease. *J. Cell Biol.* **172**, 605-618.

Ravikumar, B., Duden, R. and Rubinsztein, D. C. (2002). Aggregate-prone proteins with polyglutamine and polyalanine expansions are degraded by autophagy. *Hum. Mol. Genet.* **11**, 1107-1117.

Ravikumar, B., Vacher, C., Berger, Z., Davies, J. E., Luo, S., Oroz, L. G., Scaravilli, F., Easton, D. F., Duden, R., O'Kane, C. J. et al. (2004). Inhibition of mTOR induces autophagy and reduces toxicity of polyglutamine expansions in fly and mouse models of Huntington disease. *Nat. Genet.* **36**, 585-595.

Rubinsztein, D. C. (2002). Lessons from animal models of Huntington's disease. *Trends Genet.* **18**, 202-209.

Rubinsztein, D. C., Gestwicki, J. E., Murphy, L. O. and Klionsky, D. J. (2007). Potential therapeutic applications of autophagy. *Nat. Rev. Drug Discov.* **6**, 304-312.

Ryder, E., Blows, F., Ashburner, M., Bautista-Llacer, R., Coulson, D., Drummond, J., Webster, J., Gubb, D., Gunton, N., Johnson, G. et al. (2004). The DrosDel collection: a set of P-element insertions for generating custom chromosomal aberrations in Drosophila melanogaster. *Genetics* **167**, 797-813.

Sarkar, S., Floto, R. A., Berger, Z., Imarisio, S., Cordenier, A., Pasco, M., Cook, L. J. and Rubinsztein, D. C. (2005). Lithium induces autophagy by inhibiting inositol monophosphatase. *J. Cell Biol.* **170**, 1101-1111.

Sarkar, S., Davies, J. E., Huang, Z., Tunnacliffe, A. and Rubinsztein, D. C. (2007). Trehalose, a novel mTOR-independent autophagy enhancer, accelerates the clearance of mutant huntingtin and alpha-synuclein. *J. Biol. Chem.* **282**, 5641-5652.

Satoh, A., Wang, Y., Malsam, J., Beard, M. B. and Warren, G. (2003). Golgin-84 is a rab1 binding partner involved in Golgi structure. *Traffic* **4**, 153-161.

Shibata, M., Lu, T., Furuya, T., Degterev, A., Mizushima, N., Yoshimori, T., MacDonald, M., Yankner, B. and Yuan, J. (2006). Regulation of intracellular accumulation of mutant Huntingtin by Beclin 1. *J. Biol. Chem.* **281**, 14474-14485.

Shin, H. W., Hayashi, M., Christoforidis, S., Lacas-Gervais, S., Hoepfner, S., Wenk, M. R., Modregger, J., Uttenweiler-Joseph, S., Wilm, M., Nystuen, A. et al. (2005). An enzymatic cascade of Rab5 effectors regulates phosphoinositide turnover in the endocytic pathway. *J. Cell Biol.* **170**, 607-618.

Stenmark, H., Parton, R. G., Steele-Mortimer, O., Lutcke, A., Gruenberg, J. and Zerial, M. (1994). Inhibition of rab5 GTPase activity stimulates membrane fusion in endocytosis. *EMBO J.* **13**, 1287-1296.

Suzuki, K., Kirisako, T., Kamada, Y., Mizushima, N., Noda, T. and Ohsumi, Y. (2001). The pre-autophagosomal structure organized by concerted functions of APG genes is essential for autophagosome formation. *EMBO J.* **20**, 5971-5981.

Webb, J. L., Ravikumar, B., Atkins, J., Skepper, J. N. and Rubinsztein, D. C. (2003). Alpha-Synuclein is degraded by both autophagy and the proteasome. *J. Biol. Chem.* **278**, 25009-25013.

Wucherpfennig, T., Wilsch-Brauninger, M. and Gonzalez-Gaitan, M. (2003). Role of Drosophila Rab5 during endosomal trafficking at the synapse and evoked neurotransmitter release. *J. Cell Biol.* **161**, 609-624.

Wyttenbach, A., Swartz, J., Kita, H., Thykjaer, T., Carmichael, J., Bradley, J., Brown, R., Maxwell, M., Schapira, A., Orntoft, T. F. et al. (2001). Polyglutamine expansions cause decreased CRE-mediated transcription and early gene expression changes prior to cell death in an inducible cell model of Huntington's disease. *Hum. Mol. Genet.* **10**, 1829-1845.